THE MOHR DIAGRAM AND COULOMB EQUATION

NORMAN W. McLEOD, *Engineering Consultant, Department of Transport, Ottawa, Canada*

SYNOPSIS

Reference is made to the current difference of opinion that appears to exist concerning the significance of the Coulomb equation, the Mohr diagram, and the relationship between them. The paper reviews the simplest case, the stressing of certain soils or similar materials for which the Coulomb, principal stress, and Mohr envelopes are straight lines. Two principal conclusions are presented. The Coulomb envelope resulting from direct shear test data, and the Mohr envelope obtained from triaxial data will be identical for a given material, provided that identical samples of the material are subjected to identical conditions during both tests. Theories of stability for these materials that are based exclusively on either the principal stresses, or on relationships between normal stress, shearing stress, and shearing resistance, or on the angle of internal friction, or on the angles between the plane of failure and the major or minor principal planes, or on combinations of two or more of these, are actually supplementary theories that provide identical solutions to any stability problem concerning these materials.

Because of the increasing interest in the use of the triaxial test for the solution of highway and airport engineering problems, it is important that agreement should be reached regarding the significance of the Mohr diagram for the analysis of triaxial data, and concerning the nature of the relationship between the Coulomb and Mohr diagrams. The paper is intended to promote discussion having these objectives in view.

In spite of the many references to the Coulomb equation and Mohr diagram that occur in the technical literature on soil mechanics, and to the relationships between the two that have been pointed out, there does not yet seem to be complete agreement concerning their significance (*1*).[1]

The increasing application of the triaxial test to the solution of problems in subgrade, base course, and flexible pavement design in the fields of highway and airport engineering in particular, and in soil mechanics in general, has attracted much attention to the utility of the Mohr diagram for the analysis of triaxial data. Consequently, it is highly desirable that agreement should be reached regarding the significance of the Mohr diagram for this purpose, and concerning the relationships between corresponding Mohr and Coulomb diagrams. It is the principal intention of this paper to promote discussion having these objectives in mind.

To initiate this discussion, the writer will present a brief outline of his own understanding of several important fundamentals pertaining to the Coulomb equation, the Mohr diagram, and the relationships between them, based largely upon several different sources of information (*2*, *3*, *4*, *5*, *6*).

This presentation will be limited to the simplest case, and it pertains to the stressing of certain soils or similar materials for which it is assumed that:

1. The relationships between the stresses on the various planes through a point conform with the laws of engineering mechanics;
2. The stress data for failure conditions can be represented by straight line Coulomb, principal stress, and Mohr envelopes;
3. The materials possess both cohesion and internal friction;
4. The values determined for c and ϕ are the same for every plane through the point, or through a loaded element of the material;
5. The values determined for c and ϕ are independent of any state of stress to which the material may have been subjected before being loaded to failure.

[1] Italicized figures in parentheses refer to the references listed at the end of the paper.

Unless the assumptions on which it is to be based are clearly defined, rational debate concerning the significance of the Coulomb and Mohr diagrams and the relationships between them is likely to be difficult, because of the lack of any common basis for comparing and evaluating the different points of view.

The first assumption above is made in textbooks on engineering mechanics, and merely states, for example, that there is a definite

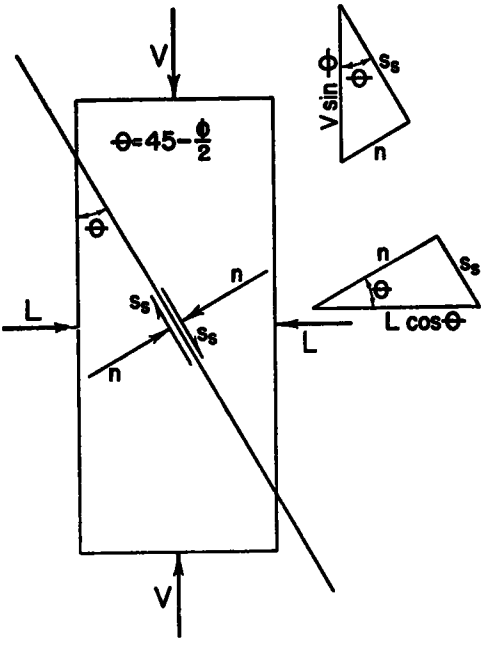

Figure 1. Principal, Shear and Normal Stresses in a Loaded Element

relationship between the principal stresses acting on the principal planes through a point, and the shear and normal stress on any other plane through the point.

While several theories, e.g. maximum normal stress theory, maximum normal strain theory, maximum shearing stress theory, etc., have been proposed to explain the failure of different substances under load, textbooks on soil mechanics seem to generally agree that the Coulomb internal friction theory provides the best explanation for the failure of soil materials. Even when the shear and normal stress data plot as a curved line, the best straight line is frequently drawn through the points to facilitate the solution of practical problems. While the Mohr theory of failure is also based on the internal friction concept, it is more general than the Coulomb theory It leaves the nature of the relationship between shear and normal stress to be determined experimentally, and does not specify that the Mohr envelope must necessarily be a straight line, as required by the Coulomb equation, $s = c + n \tan \phi$. Nevertheless, carefully obtained shear and normal stress data for many soils do seem to plot as straight lines, and for these the assumption of straight line Coulomb, principal stress, and Mohr envelopes appears to be justified.

Certain cohesive soils lack internal friction, and have Coulomb or Mohr envelopes that are parallel to the abscissa. Cohesionless soils, such as sands and gravels, possess internal friction, and when they are completely lacking in cohesion, their Coulomb or Mohr envelopes tend to pass through the origin. A great many of the soils and flexible base and pavement materials with which the highway and airport engineer is concerned possess both cohesive and internal friction properties. These latter materials are considered in this paper to represent the general case.

It should be emphasized again, that the subject matter of this paper is limited to a discussion of the Coulomb and Mohr diagrams and the relationships between them for the simplest case of comparison, which is confined to stressed soil or similar materials to which the five listed assumptions apply.

Throughout the text and diagrams, all forces are considered to be unit stresses in pounds per square inch or similar strength units.

STRESSES IN A LOADED ELEMENT

While the term "stresses at a point" is frequently employed in textbooks on mechanics, it is usual practice to enlarge the "point" to a small two or three dimensional element. Relationships between stresses on planes through this small element can be more easily visualized than on planes through a point.

Figure 1 represents a small element of soil subjected to principal stresses V and L. If the lateral pressure L is maintained constant while the vertical load V is gradually increased, failure will eventually occur along one of the planes through the element. If the angles between various planes through the element and the vertical are designated by

different values of θ, then from the Coulomb theory of failure, it follows that the particular value of θ for the plane of failure is given by $\theta = 45 - \frac{\phi}{2}$, where ϕ is the angle of internal friction for the material.

Application of the principal stresses V and L develop shearing stresses s_s and normal stresses n on all planes through the element. The shearing and normal stresses developed on the plane of failure are shown in Figure 1.

It is clear from Figure 1 that the shear stress s_s acting along any plane through the element is the algebraic sum of the components of the principal stresses V and L acting along that plane. Similarly, the normal stress n acting on any plane through the element is the algebraic sum of the components of V and L acting at right angles to that plane. Consequently, there is a very close relationship between the principal stresses acting on an element, and the shear and normal stresses developed on any plane through the element, and vice versa. Therefore, from triaxial data which provide corresponding values of V and L for the condition of incipient failure of the element, the values of the corresponding component shear and normal stresses s_s and n developed on the plane of failure can be calculated. Conversely, from direct shear test data which provide corresponding values of s_s and n for incipient failure conditions along the plane of failure through the material, the corresponding principal stresses V and L can be calculated.

Chronologically, the direct shear test is much older than the triaxial test, and it will be discussed first.

DIRECT SHEAR TEST AND COULOMB ENVELOPE

The small rectangular box around a portion of the plane of failure in Figure 2 (a) attracts attention to the fact that although the stresses applied to the loaded specimen during a direct shear test are the shearing stress s_s and the normal stress n on the plane of failure, they are closely related to the corresponding principal stresses V and L.

Figure 2 (b) illustrates the principle of the direct shear test. One of its most common forms is the shear box in which the material to be tested is placed. The top half of the shear box is displaced relative to the bottom half, subjecting the specimen to shear along the plane between the two halves of the box. A normal stress n of some given magnitude is applied as shown, and the shear stress s_s that causes failure is determined. The test is repeated on other similar specimens of the same material to each of which a different normal stress is applied. The resulting normal and shear stress data for the failure condition are plotted as shown in Figure 2(c). The straight line through the data is called the Coulomb envelope. Its intercept with the ordinate axis is known as cohesion c, while the angle between the Coulomb envelope and the horizontal is the angle of internal friction ϕ. The Coulomb envelope, therefore, is a graphical representation of the Coulomb equation,

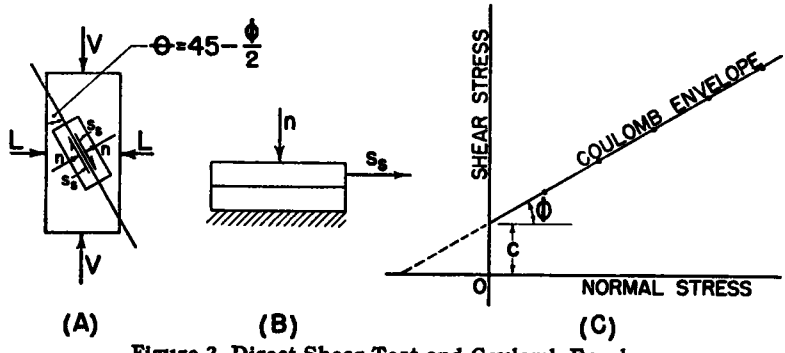

Figure 2. Direct Shear Test and Coulomb Envelope

$$s_r = c + n \tan \phi \qquad (1)$$

where s_r = shearing resistance of the material, and the other symbols have the significance already explained for them. It should be apparent that for equilibrium (incipient failure) conditions, for any given

normal stress n, the maximum shearing stress s_s that can be applied on the plane of failure must be equal to the shearing resistance s_r of the material that can be developed on that plane.

Incidentally, much of the debate concerning the significance of the intercept made by the Coulomb envelope with the ordinate axis, which has come to be known as cohesion c, might be simplified if it were always kept in mind that this intercept actually represents the maximum shearing resistance that can be developed by the material under the condition of zero normal stress, as the Coulomb diagram Fig. 2(c) indicates.

For many soil materials, a plot of s_s versus n from direct shear test data results in a curved line rather than the straight line envelope shown in Figure 2(c). However, as emphasized in the introduction, this paper is concerned with only the latter case.

The portion of the Coulomb envelope to the right of the ordinate axis in Figure 2(c) can be easily determined by direct shear test data, because the applied normal stresses n are acting in compression. The smallest normal stress that can ordinarily be applied to a soil specimen during a laboratory direct shear test is $n = 0$. This is indicated by the ordinate axis in Figure 2(c).

Because of the nature of soil materials, it would be difficult to apply uniform tensile stresses to them in the laboratory. For this reason, it is not possible to check the position of the Coulomb envelope to the left of the ordinate axis, since this would require the application of negative uniform normal pressure during the direct shear test, that is, normal stress acting in tension. Consequently, the portion of the Coulomb envelope to the left of the ordinate axis in Figure 2(c) and in subsequent diagrams has been shown as a broken line, to emphasize that its exact position has not been experimentally verified by actual data on soil materials. This left-hand broken line portion has been shown as a continuous projection of the part of the Coulomb envelope on the right of the ordinate axis, merely because for materials such as concrete and steel, to which tensile stresses can be applied, the position of the Coulomb envelope on each side of the ordinate axis has been established by actual test data (Fig. 6). It is to be emphasized that our inability to check the position of the portion of the Coulomb envelope to the left of the origin for soil materials, is due to our being unable to devise suitable laboratory apparatus for this purpose. It does not mean that normal stresses acting in tension do not occur in nature, or in actual engineering structures in the field, under certain conditions.

Having obtained the straight line Coulomb envelope of Figure 2(c), the next step is to locate the position of the principal stresses V and L on this diagram, if possible.

Figure 3 emphasizes the fact that s_s and n are components of the principal stresses V and L, and that although only the shear stress s_s and normal stress n are actually applied to the specimen and measured in a direct shear test, the existence of the corresponding principal stresses V and L is implied, when this test is made.

The loaded elements in Figure 3(a), (d), (g), and (j), show the principal, normal, and shear stresses acting under each of four separate conditions of stress. The direct shear test diagrams of Figure 3(b), (e), (h), and (k) illustrate the shear stress s_s and normal stress n acting in each of these four cases, and also the directions in which the implied corresponding principal stresses V and L are acting. The direct shear test diagrams in Figure 3(b), (e), (h), and (k) have been drawn in an oblique position parallel to the direction of the planes of failure in Figure 3(a), (d), (g), and (j), respectively. This places the principal, shear, and normal stresses in parallel positions and directions in both sets of diagrams, and makes them easier to follow.

About seventy years ago, Mohr (7) demonstrated a method whereby the magnitude and direction of the corresponding principal stresses V and L can be obtained, if the shear stress s_s and normal stress n have been determined for equilibrium (incipient failure) conditions. A point representing the coordinates of any given combination of shear and normal stress is marked on the Coulomb envelope, e.g. point P in Figure 3(c). Through this point a semi-circle is drawn to which the Coulomb envelope is tangent, and that has its diameter along the normal stress axis. The points of intersection of the semi-circle with the normal stress axis represent the values of the principal stresses V and L corresponding to the shear and normal stresses indicated by the point P. No assumptions are involved in this graphical procedure, and the proof that

it gives precisely the same relationships concerning principal, shear, and normal stresses, angle of failure θ, etc., that can be derived from a consideration of the stresses acting on the loaded element of Figure 1 or Figure 3(a), etc., will be given later in connection with Figure 12.

illustrated by Figure 3 (g), (h), and (i), in which the shear stress s_s, and major principal stress V are positive, but the minor principal stress L is negative. That is, L acts in tension. Figure 3(j), (k), and (l) pertain to Case (4), which represents the tensile strength condition. The shear stress s_s is positive and $V = 0$,

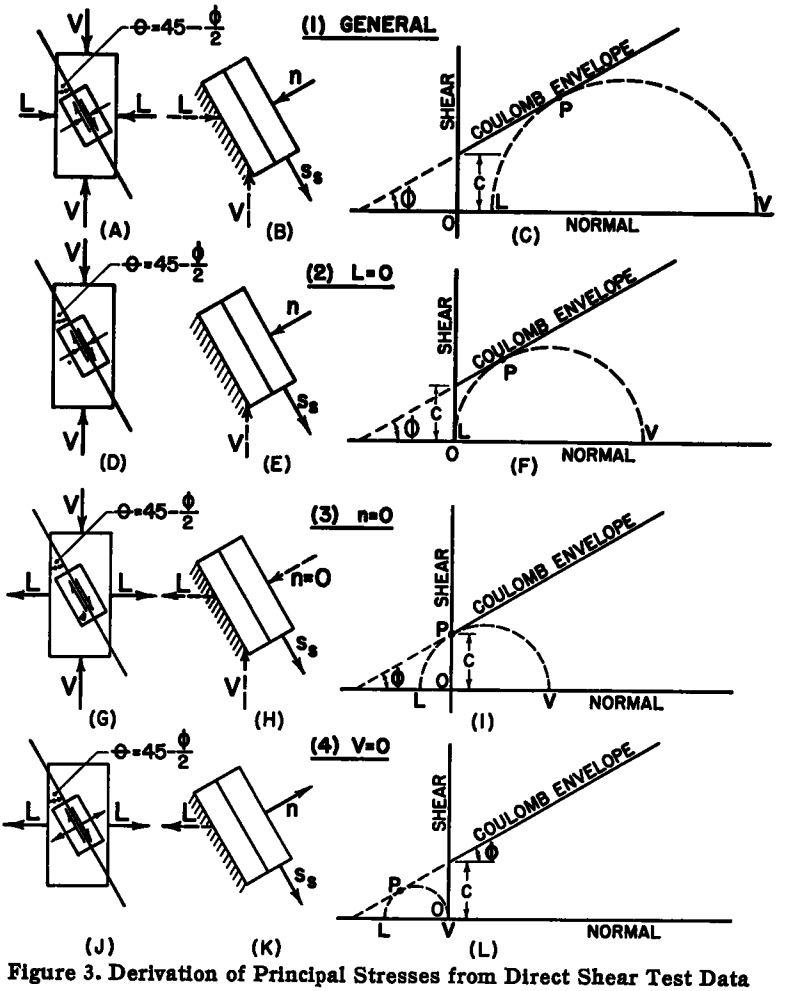

Figure 3. Derivation of Principal Stresses from Direct Shear Test Data

Figure 3(c), therefore, provides a graphical representation of the magnitude of, and relationships between the principal, shear, and normal stresses acting in Figure 3(a) and (b) for Case (1), where s_s, n, V, and L are all positive. Figure 3(d), (e), and (f) relate to the stress conditions in Case (2), which pertain to unconfined compression, where s_s, n, and V are positive, but $L = 0$. Case (3), covering the condition where the normal stress $n = 0$, is while both n and L are negative, that is, acting in tension.

It should be carefully observed again that due to the limitations of present laboratory equipment, the stress conditions represented by Case (4) cannot be experimentally verified for soil materials, because of the tensile normal stress involved. However, direct shear tests covering Cases (1), (2), and (3) of Figure 3 can be quite readily conducted in the labora-

tory. Of particular interest is Case (3), in which the normal stress $n = 0$, and for which the corresponding minor principal stress L is negative, and, therefore, acts in tension.

TRIAXIAL TEST AND MOHR DIAGRAM

In the triaxial test, shown diagramatically in Figure 4(a), a cylindrical specimen, to which a lateral pressure L is applied, is subjected to increasing vertical load V until it fails. Similar specimens are tested in like manner at other magnitudes of lateral pressure L. The resulting corresponding values of V and L can be plotted in the form of a principal stress diagram, Figure 4(b). For this paper, only those soil and flexible pavement materials are considered that provide the straight line relationship between V and L that is illustrated in Figure 4(b).

Using the V and L values either provided directly by the triaxial tests, or taken from the straight line relationship of Figure 4(b), Mohr circles can be drawn as shown in Figure 4(c). For this purpose, the corresponding values of V and L in each case are laid off along the normal stress axis, and the difference between them, $V - L$, forms the diameter of a semi-circle known as a Mohr circle.

It is apparent from the straight line relationship of Figure 4(b), that an infinite number of corresponding values of V and L could be selected. When a large number of these are taken and plotted on a Mohr diagram, the Mohr circles of Figure 4(d) result. When an infinite number of these corresponding values of V and L are selected, the resulting Mohr circles are so close together that the Mohr diagram of Figure 4(e) is obtained. The top boundary provided by the Mohr circles of Figure 4(e) forms a straight line known as the Mohr envelope, which is obviously tangent to each of the Mohr circles.

It will be observed that the left-hand extremity of the Mohr envelope in Figures 4(d) and (e) is marked by its point of tangency with the Mohr circle representing the unconfined compressive strength, for which the lateral pressure $L = 0$. One should be on his guard, however, against any interpretation that the Mohr envelope either terminates or changes its direction at this point. It merely means that with present triaxial equipment it is not possible to explore the position of the Mohr envelope toward the left beyond its point of tangency with the Mohr circle representing the unconfined compressive strength. This is due to our present inability to apply uniform negative lateral pressures L (that is, L acting in tension), to soil specimens in the triaxial test. To establish experimentally the position of the Mohr envelope to the left of its point of tangency with the Mohr circle representing the unconfined compressive

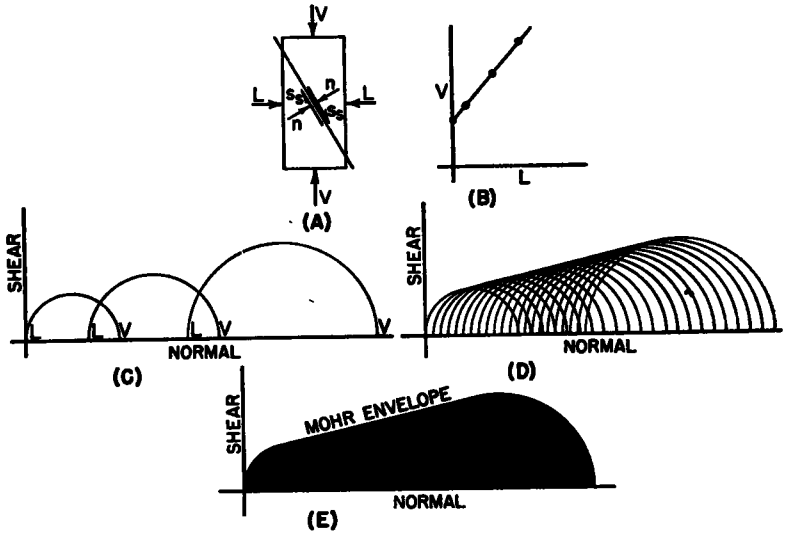

Figure 4. Principal Stress and Mohr Diagrams

strength, by means of the triaxial test, it is apparent that Mohr circles farther to the left would be required, and the experimental data needed for these could only be obtained if uniform negative lateral pressures L could be applied.

Soil stresses in nature are not subject to the limitations of the triaxial test, and stress conditions undoubtedly occur sometimes in the field that correspond to those represented by extending the Mohr envelope of Figure 4(e) toward the left. The justification for this

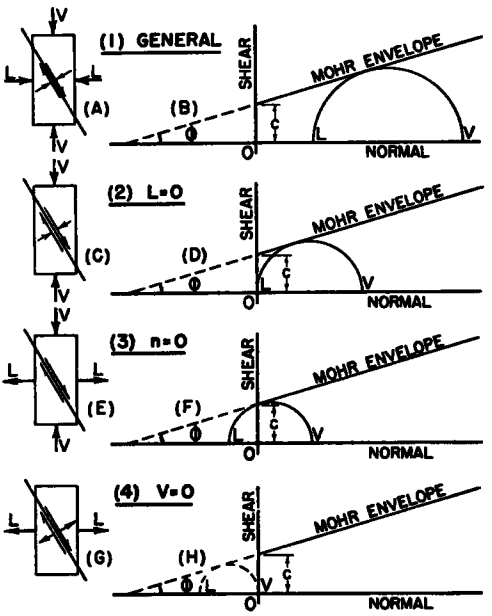

Figure 5. Mohr Diagrams for Different Conditions of Loading

can be more clearly understood from a study of the four cases portrayed diagrammatically in Figure 5.

Case (1) of Figure 5 covers the general condition where both vertical stress V and lateral pressure L are acting in compression. Case (2) portrays the nature of the stresses involved for unconfined compression, when the minor principal stress $L = 0$. Case (3) pertains to a condition of loading that would be difficult to obtain in the triaxial testing of soils, because it requires that the minor principal stress L must act in tension. The V and L stresses are so selected that the normal pressure n on the plane of failure is zero ($n = 0$), as Figure 5(f) indicates. While Case (3) of Figure 5 would be very difficult to approximate with triaxial equipment, it will be recalled from Case (3) of Figure 3 that the stress conditions involved can be attained quite easily by means of the direct shear test. This justifies the extension of the Mohr envelope to at least the point of its intersection with the ordinate axis. Case (4) of Figure 5 illustrates the tensile strength condition. The stress conditions represented by Case (4) cannot be checked experimentally for soil materials, because present triaxial laboratory equipment cannot uniformly apply the tensile stresses required. Therefore, the portion of the Mohr envelope to the left of the ordinate axis in Figure 5 and in subsequent diagrams has been shown as a broken line.

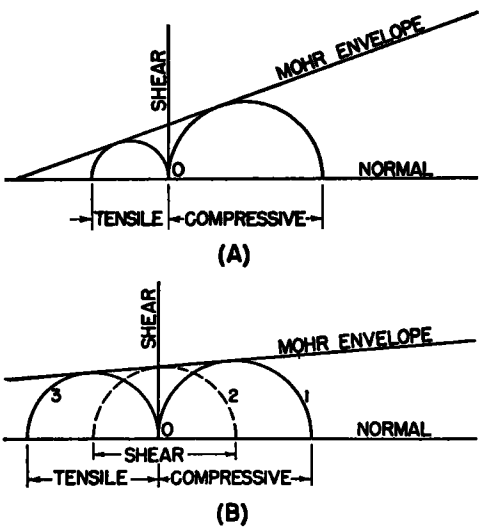

Figure 6. Mohr Diagrams for Concrete and Steel

While it cannot be checked for soil materials, the Mohr diagram of Case (4) has been established for certain other substances such as concrete, cast iron, metals, etc., when tested in simple tension. This is illustrated by the Mohr diagrams of Figure 6 for concrete and steel. The Mohr circle on the right-hand side of the origin in each case in Figure 6 represents the compressive strength of the material, while that on the left-hand side is for the tensile strength condition. In Figure 6(b), a Mohr circle is shown that corresponds to the shearing resistance of steel at zero normal stress obtained from a direct shear test. Consequently, in Figure 6(b), Mohr circle (1) was derived from the compressive strength of

steel, Mohr circle (2) from its shearing strength and Mohr circle (3) from its tensile strength.

As shown in Figure 5(b), (d), (f), and (h), the Mohr envelope makes an intercept with the ordinate axis known as cohesion c, while the angle between the Mohr envelope and the horizontal is the angle of internal friction ϕ. The similarity between the Mohr envelopes and the diagrams of Figure 5(b), (d), (f), and (h), and the Coulomb envelopes and the diagrams of Figure 3(c), (f), (i), and (l), is quite apparent.

to the shearing resistance s_r for the given sample of material, and for the particular normal stress n applied. The Coulomb envelope is obtained by plotting the shear stress at failure for similar specimens of the same material tested at other normal pressures, and drawing a straight line through the points so obtained.

In Case (2) of Figure 7, the specimen is subjected to a constant lateral support L in triaxial equipment, and vertical stress V is applied in increments, or as a gradually in-

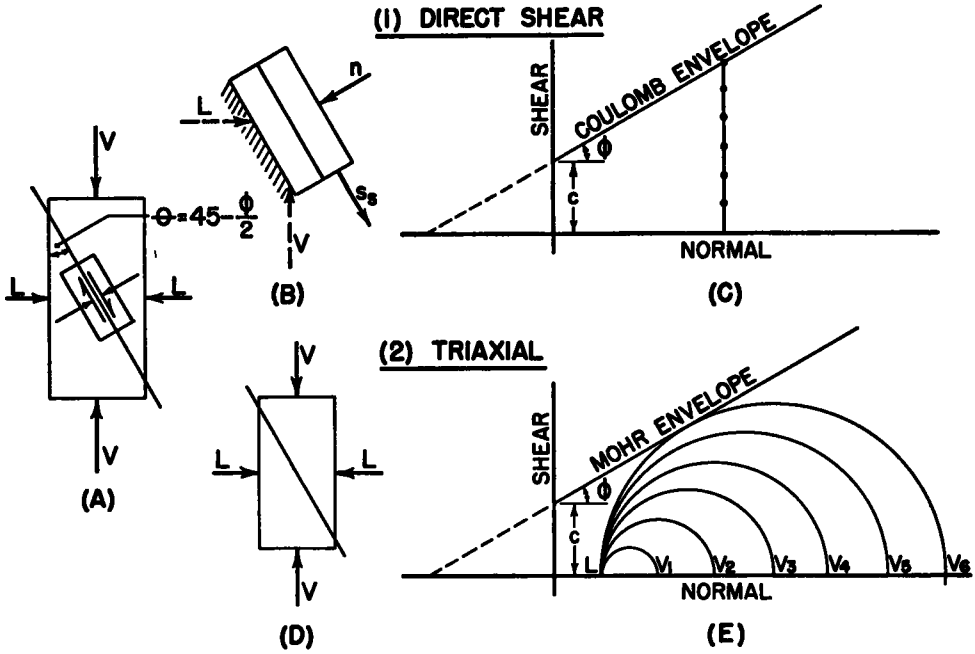

Figure 7. Illustrating the Derivation of Coulomb and Mohr Envelopes for a Given Soil Material

COMPARISON OF COULOMB AND MOHR ENVELOPES

Figure 7 illustrates the manner in which actual data are obtained for both direct shear and triaxial tests. In Case (1) for the direct shear test, the specimen is subjected to a constant normal stress n, while shear stress s_s is applied in increments or as a gradually increased load until the shearing resistance of the material at that normal pressure is reached, when shear failure occurs. This is illustrated by the vertical line in Figure 7(c). The intersection of this vertical line with the Coulomb envelope represents the point where the applied shearing stress s_s is just equal

creased load, until failure of the specimen occurs. This procedure is illustrated by the successively larger Mohr circles in Figure 7(e), in which V_6 represents the largest value of vertical load that the specimen can carry without failure for the particular magnitude of lateral support L shown. Similar specimens under different values of lateral pressure L can be tested to determine other combinations of V and L that just represent failure conditions. Mohr circles can be drawn using the different corresponding values of $V - L$ as diameters. The Mohr envelope is drawn tangent to the Mohr circles for the values of V and L that represent failure conditions.

The question arises as to whether or not, for any given material, the Coulomb envelope obtained from direct shear test data is identical with the Mohr envelope derived from triaxial data (Fig. 7). It was pointed out in connection with Figure 1 that the shear stress s_s and normal stress n acting on the plane of failure are components of the principal stresses V and L. It was also pointed out that shear stress s_s and normal stress n are applied when performing the direct shear test on a given material, whereas the triaxial test makes use of the principal stresses V and L. Since the shear and normal stresses on the plane of failure are components of the principal stresses, it follows from the laws of mechanics that the Coulomb envelope for any given material must be identical with the Mohr envelope (Fig. 8(b)) provided that identical specimens of the material are tested under identical conditions in both the direct shear and triaxial tests.

Data obtained by Taylor (*8*) for several sands indicate that reasonably good agreement between the Coulomb and Mohr envelopes derived from direct shear and triaxial tests, respectively, can be obtained.

Whenever the Coulomb envelope derived from direct shear tests on a given material is different from the Mohr envelope obtained from triaxial tests on the same material (Fig. 8(a)) it is evidence that either the material has not been subjected to identical conditions in both tests, or the specimens of the material employed for each test are not identical in every respect.

It is believed that the laws of thermodynamics also require the Coulomb envelope and Mohr envelope to coincide, when identically prepared specimens are subjected to identical conditions in both direct shear and triaxial tests. If, as illustrated in Figure 9, they do not coincide, it would be possible to shear the given material in one direction by means of shear and normal stresses (direct shear), and by tilting the specimen to shear it in the reverse direction along the same plane to its initial position by means of principal stresses (triaxial shear), and repeat the process indefinitely. Since, for example, the principal stresses corresponding to the applied shear and normal stresses acting on the plane of failure in one direction would not necessarily be equal to the principal stresses employed for shearing the material in the reverse direction along the same plane to its initial position, such a system would lead to perpetual motion created and maintained by the difference between the two sets of principal stresses.

The laws of thermodynamics indicate that perpetual motion is impossible, and that conclusions regarding any system are untenable if they imply that perpetual motion would result. Consequently, identically prepared specimens tested under identical conditions in both direct shear and triaxial tests could not have the different planes of failure θ_1 and θ_2 shown in Figures 9(a) and (c), nor the different Coulomb and Mohr envelopes illustrated in Figures 9(b) and (d). That is, for the conditions concerning specimens and tests specified in the previous sentence, the planes of failure and the Coulomb and Mohr envelopes indicated by direct shear and triaxial tests on the given material must coincide.

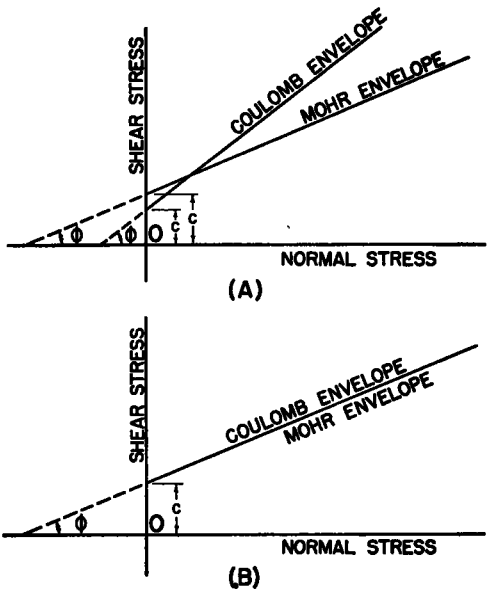

Figure 8. Relationship between Mohr and Coulomb Envelopes

Conversely, if the direct shear and triaxial data indicate that the planes of failure given by the two tests are different, and that the Coulomb and Mohr envelopes do not coincide, it is proof that either identical specimens have not been employed for each test, or that the specimens have been subjected to different conditions during the two tests.

SIGNIFICANCE OF THE MOHR DIAGRAM

In Figure 10(a), planes of shear numbered 1, 2, 3, 4, 5, and 6, through an element of material subjected to principal stresses V and L under equilibrium conditions, have been indicated. The angle θ between each of these planes and the vertical is shown. Figure 10(b) is a Mohr diagram indicating corresponding for point 5 is twice the angle θ between plane No. 5 and the vertical in Figure 10(a).

Of particular interest in Figure 10(b) is point No. 3, at which the Mohr envelope is tangent to the Mohr circle. Point 3, representing the plane for which $\theta = 45 - \frac{\phi}{2}$, indicates that the shearing stress s_s on plane

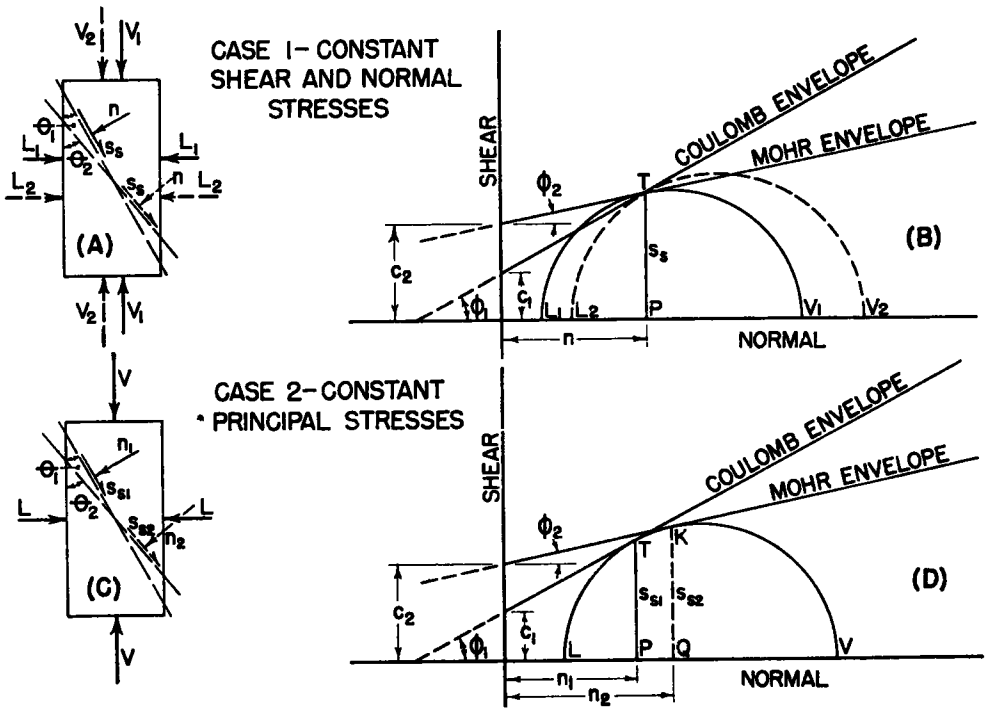

Figure 9. Illustrating the Significance of the Relationships between the Mohr and Coulomb Envelopes for a Given Material

shearing stress s_s, shearing resistance s_r, and normal stress n on each of these six planes. Thus, point 5, for example, on the Mohr circle of Figure 10(b) indicates that the normal stress n on shear plane No. 5 of Figure 10(a) is equal to OE, and that the shearing stress s_s on this plane is equal to EJ. For normal pressure OE, the corresponding shearing resistance s_r on plane No. 5 is shown by the Mohr envelope to be EN. Consequently, the shearing resistance s_r on plane No. 5 through the material is greater than the shearing stress s_s and it could not, therefore, be the plane of failure. The position of point 5 on the Mohr circle is obtained by turning off the angle 2 θ at the center as shown in Figure 10(b), where 2 θ No. 3 is just equal to the shearing resistance s_r on this plane. Both shearing stress and shearing resistance on this plane are represented by CH in Figure 10(b), and the normal pressure n is indicated by OC. Figure 10(b) demonstrates that on every other plane through the loaded element of Figure 10(a), the shearing stress s_s is less than the shearing resistance s_r represented by the Mohr envelope for the same normal pressure n. Consequently, plane No. 3 for which $\theta = 45 - \frac{\phi}{2}$, and for which shearing stress s_s is just equal to shearing resistance s_r, is the critical plane or plane of failure. Any increase in the shear

stress s_s on this critical plane, with the shearing resistance s_r remaining constant, would result in failure, since the shearing stress s_s would then exceed the shearing resistance s_r of the material.

It should be apparent that if planes of shear were also drawn through the other two quadrants of Figure 10(a), the shear and normal stresses on these planes would be indicated on the Mohr diagram of Figure 10(b), by

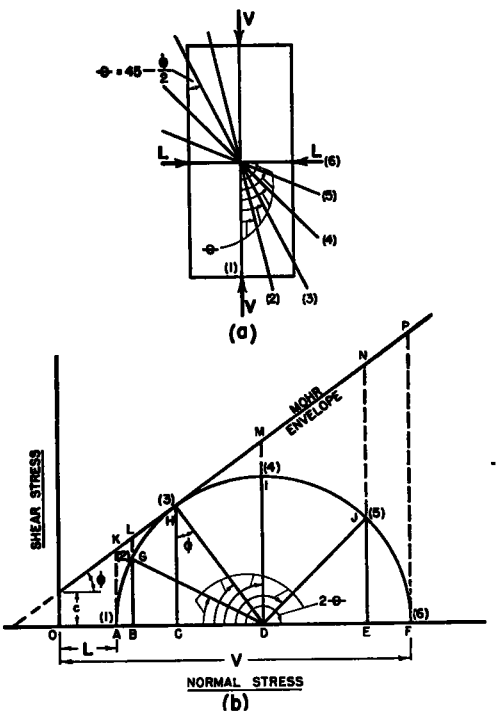

Figure 10. Illustrating the Interpretation of the Mohr Diagram

points on the circumference of a semi-circle below the abscissa. That is, the semi-circle of Figure 10(b) would become a full circle. For the half of the Mohr circle below the abscissa, points on its circumference would be coordinates of positive values of normal stress n, but negative values of shearing stress s_s. This is due to the fact that if the direction of shearing stress along the planes shown through two quadrants in Figure 10(a) is positive, then the direction of the shearing stress along planes through the other two quadrants of Figure 10(a) must be negative.

CRITERIA OF FAILURE IN TRIAXIAL LOADING

In a triaxial test, the specimen is subjected to both shear and normal, and to principal stresses. It is of value to determine whether or not failure occurs due to the difference between the principal stresses V and L applied at the time of failure, or because the shearing stress s_s exceeds the shearing resistance s_r of the material on the plane of failure.

Figure 11 illustrates three different conditions of stress that can be considered for a specimen of a given soil material tested in triaxial compression, when the lateral pressure L is maintained constant and the vertical

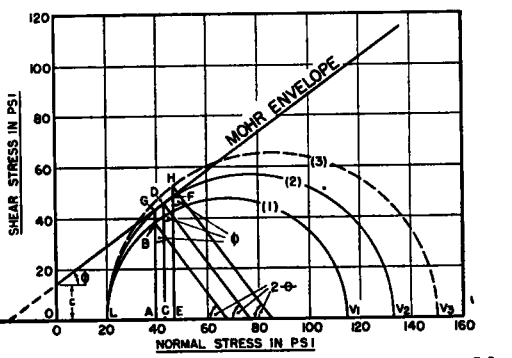

Figure 11. Mohr Circles Illustrating Stable, Equilibrium and Failure Conditions

pressure V is gradually increased. Mohr Circle (1) represents a very stable combination of loading that is materially less than the failure point. Its circumference is well below the Mohr envelope, indicating that the particular combination of principal stresses, V_1 and L, that it represents would be quite safe. According to the Coulomb theory, when failure occurs, it takes place on a plane making an angle $\theta = 45 - \frac{\phi}{2}$ with the vertical. Mohr Circle (1) indicates that the shearing stress AB generated on the plane of failure is appreciably less than the shearing resistance of the material on this plane, represented by AG. Consequently, neither the shearing stress developed on the plane of failure, nor the difference between the principal stresses V_1 and L would cause failure of the specimen under the conditions of loading represented by Mohr Circle (1).

Mohr Circle (2) of Figure 11 just touches

the Mohr envelope. Therefore, V_2 represents the largest vertical load the specimen can carry without failure for the lateral support L being supplied. Mohr Circle (2) also demonstrates that the shearing stress CD developed on the plane of failure is just equal to the maximum shearing resistance CD that can be mobilized on this plane. It is quite clear from Mohr Circle (2), therefore, that the maximum shearing stress s_s on the plane of failure and the maximum vertical load V that the specimen can sustain without failure, both develop at exactly the same time.

Mohr Circle (3) of Figure 11 represents an impossible condition of stress, and could not be developed in a test specimen. Mohr Circle (3) cuts through the Mohr envelope and, therefore, indicates a value of vertical load V_3 that could not be obtained for the given degree of lateral support L provided, because the specimen would fail before it had been reached. It should also be noted that the shearing stress EH that would be generated on the plane of failure for the conditions of loading represented by Mohr Circle (3) would be greater than the maximum shearing resistance EF that can be developed on this plane. Thus, Mohr Circle (3) represents an impossible condition of loading from the point of view of both the shearing stress and the principal stresses involved, and it has, therefore, been drawn with a broken line.

Figure 11 demonstrates that when a definite quantity of lateral support L is provided for a specimen that is loaded triaxially, failure will occur when the major principal stress V exceeds a certain critical value, V_2 in Figure 11. It also clearly indicates that when the major principal stress exceeds the critical value V_2, the shearing stress on the critical plane simultaneously exceeds the maximum shearing resistance that can be developed on that plane. It should be recalled again in this connection that the shear and normal stresses on any plane through a point are components of the principal stresses acting at that point. Consequently, it cannot be said that failure of the specimen is due singly either to the difference between the principal stresses V and L, or because the shearing stress exceeds the shearing resistance on the critical plane. Since each of these two factors is effective at precisely the same time, both are criteria of failure. Unless this were true, shearing resistance could not be measured by the triaxial test. Therefore, theories of stability for soil and flexible pavement materials that are based exclusively on either the relationship between the principal stresses, or the ratio of shearing stress to shearing resistance on the plane of failure, are supplementary and closely interrelated approaches that provide identical solutions to stability problems pertaining to these materials.

EQUATIONS OF STRESS FOR A LOADED ELEMENT

Figure 12(a) indicates the stresses and the angles of inclination of the plane of failure to both the vertical and horizontal planes, between which relationships are frequently required for the condition of incipient failure (equilibrium) of a loaded element. All of the quantities shown have been previously defined except α, which is the angle between the plane of failure and the horizontal.

Figure 12(b) is a principal stress diagram for a material for which the relationship between the major and minor principal stresses can be represented by a straight line. The limited usefulness of this diagram for visually illustrating the magnitudes of the various stresses and angles shown in Figure 12(a) is obvious.

Figure 12(c) is a Mohr diagram corresponding to the principal stress diagram of Figure 12(b). The outstanding advantages of the Mohr diagram are quite evident. The relative magnitudes of the quantities V, L, s_r, s_s, n, θ, and α shown in Figure 12(a) are visually and immediately apparent from even a cursory examination of the Mohr diagram. In addition, the Mohr diagram develops and illustrates the magnitudes of the cohesion c and the angle of internal friction ϕ, which are properties of the material that are not even indicated by the diagrams of Figure 12(a) and (b). That no assumptions are made when going from either Figure 12(a) or Figure 12(b) to the Mohr diagram of Figure 12(c) is quite clear from the fact that precisely the same relationships can be derived from the Mohr diagram that can be established from a consideration of the stresses acting on the loaded element of Figure 12(a). This is illustrated in Figure 12 for the shear stress s_s and the normal stress n, for which it will be observed that identical equations can be derived on the basis of either the loaded element of Figure 12(a), or the Mohr diagram of Figure 12(c). The Mohr diagram of Figure 12(c) is a precise graphical method for

illustrating the size of the angles involved, and the magnitudes of the various stresses acting on the loaded element of Figure 12(a).

For a soil or similar material for which stress conditions can be represented by straight line Coulomb, principal stress, and Mohr envelopes, that has both cohesion and internal friction characteristics, and that meets the other assumptions specified in the introduction, the following equations can be written to express equilibrium relationships between the principal stresses V and L, in terms of θ,

$$s_s = L \sin \phi \sqrt{\frac{1 + \sin \phi}{1 - \sin \phi}} + c(1 + \sin \phi) \quad (7)$$

For the developed normal stress, the equations in terms of each of the three angles are:

$$n = 2L \cos^2 \theta + c \sin 2\theta \quad (8)$$
$$n = 2L \sin^2 \alpha + c \sin 2\alpha \quad (9)$$
$$n = L(1 + \sin \phi) + c \cos \phi \quad (10)$$

Theories of stability for soil materials have been built up around the angle of internal friction ϕ (Coulomb's internal friction theory),

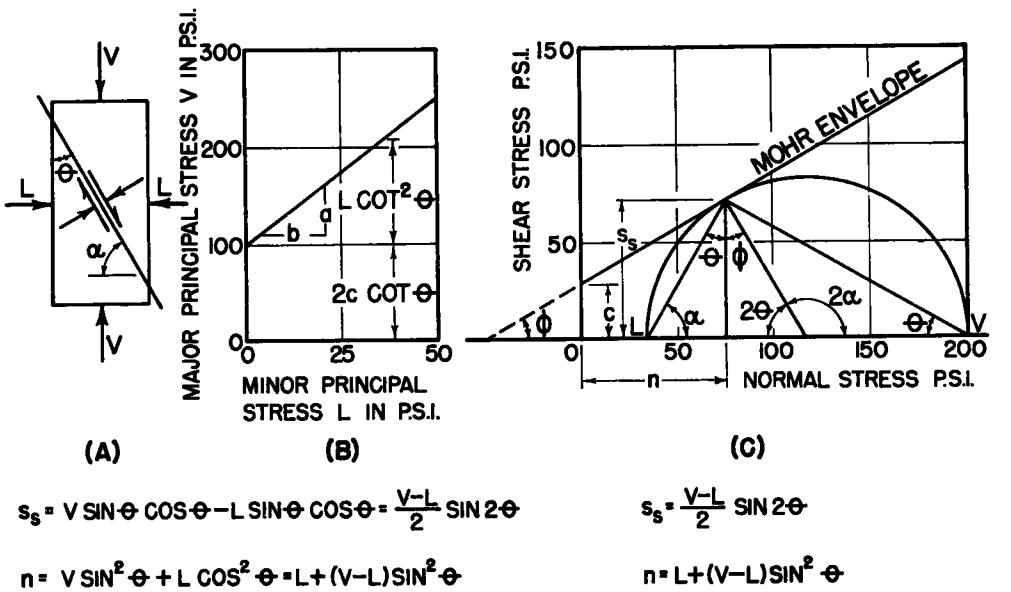

Figure 12. Illustrating Identity of Stress Relationships Derived from a Loaded Element and from the Corresponding Mohr Diagram

the angle between the plane of failure and the vertical, α, the angle between the plane of failure and the horizontal, and ϕ, the angle of internal friction:

$$V = L \cot^2 \theta + 2c \cot \theta \quad (2)$$
$$V = L \tan^2 \alpha + 2c \tan \alpha \quad (3)$$

$$V = L\left(\frac{1 + \sin \phi}{1 - \sin \phi}\right) + 2c\sqrt{\frac{1 + \sin \phi}{1 - \sin \phi}} \quad (4)$$

The equations for the developed shear stress in terms of the three angles are:

$$s_s = L \cot \theta \cos 2\theta + 2c \cos^2 \theta \quad (5)$$
$$s_s = -L \tan \alpha \cos 2\alpha + 2c \sin^2 \alpha \quad (6)$$

and also around either the angle θ (Housel's arching action theory) (9) between the plane of failure and the vertical (minor principal plane), or the angle α between the plane of failure and the horizontal (major principal plane). However, there is a complementary relationship between these three angles as shown below:

$$\theta = 45 - \frac{\phi}{2} \quad (11)$$

$$\alpha = 45 + \frac{\phi}{2} \quad (12)$$

$$\theta = 90 - \alpha \quad (13)$$

Consequently, a theory of stability based upon one of these three angles is supplementary to a theory of stability built up around either of the other two angles. These theories are, therefore, essentially identities, and they will give identical solutions to any given stability problem concerning these materials.

Therefore, theories of stability for soil materials that are based exclusively on either the principal stresses, or on relationships between normal stress, shearing stress, and shearing resistance, or on the angle of internal friction, or on either of the angles between the plane of failure and the major or minor principal planes, or on combinations of two or more of these, are actually supplementary theories that provide identical solutions to any stability problem concerning these materials. As previously pointed out, corresponding direct shear and triaxial test data that seem to indicate fundamental differences between these theories of stability for soil materials, merely provide evidence that either the test specimens were not identical, or they were not subjected to identical conditions in the direct shear and triaxial equipment employed to provide the test data.

SUMMARY

1. There appears to be some difference of opinion at the present time concerning the significance of the Mohr diagram when used for the analysis of triaxial data, and regarding the relationships between the Coulomb and Mohr diagrams.

2. The characteristics of the Coulomb diagram employed for direct shear test data are described.

3. The use of the Mohr diagram for the analysis of triaxial data is reviewed.

4. For given soil materials tested under identical conditions in direct shear and triaxial equipment, it is shown that the Coulomb and Mohr envelopes must be identical.

5. The criteria of failure involved when a specimen is loaded triaxially to failure are examined.

6. The conclusion is reached that theories of stability for given soil or similar materials, that are based exclusively on either the principal stresses, or on relationships between normal stress, shearing stress, and shearing resistance, or on the angle of internal friction, or on either of the angles between the plane of failure and the major or minor principal planes, or on combinations of two or more of these, are actually supplementary theories, or identities, that provide identical solutions to any stability problem concerning these materials.

7. Corresponding direct shear and triaxial test data that seem to indicate fundamental differences between these theories of stability for the given materials, merely provide evidence that either the test specimens were not identical, or they were not subjected to identical conditions in the direct shear and triaxial equipment employed to provide the test data.

ACKNOWLEDGEMENTS

The material presented in this paper is related to an extensive investigation of Canadian airports that was undertaken by the Canadian Department of Transport early in 1945. Air Vice-Marshall A. T. Cowley, Director of Air Services, has the general administration of this investigation. It comes under the direct administration of Mr. Harold J. Connolly, Superintendent Construction, Mr. George W. Smith, Assistant Superintendent Construction, and Mr. E. B. Wilkins. In their respective districts the investigation is carried on with the generous co-operation of District Airway Engineers T. Chillcott, E. F. Cooke, John H. Curzon, Frank Davis, Oliver Kelley, and W. G. D. Stratton.

REFERENCES

1. W. S. Housel, "Interpretation of Triaxial Compression Tests of Granular Mixtures," *Proceedings*, The Association of Asphalt Paving Technologists, Volume 19 (1950).
2. Karl Terzaghi, "Theoretical Soil Mechanics," John Wiley and Sons Inc., New York (1944).
3. Donald W. Taylor, "Fundamentals of Soil Mechanics," John Wiley and Sons Inc., New York (1948).
4. D. P. Krynine, "Soil Mechanics," McGraw-Hill Book Company Inc., New York (1947).
5. Karl Terzaghi and Ralph B. Peck, "Soil Mechanics in Engineering Practice," John Wiley and Sons Inc., New York (1948).
6. Glenn Murphy, "Advanced Mechanics of Materials," McGraw-Hill Book Company Inc., New York (1946).
7. O. Mohr, "Uber die Darstellung des Spannungszustandes und des Deformationzustandes eines Korper-elements," *Zivilingenieur*, p. 113, 1882.

8. D. W. Taylor, "A Comparison of Results of Direct Shear and Cylindrical Compression Tests," *Proceedings*, American Society for Testing Materials, Vol 39 (1939).

9. W. S. Housel, "Internal Stability of Granular Materials," *Proceedings*, American Society for Testing Materials, Vol. 26, Part 2 (1936).

STUDIES OF THE CLAY FRACTION IN ENGINEERING SOILS

W. E. HAUTH, JR., *Assistant Professor of Ceramic Engineering* AND DONALD T. DAVIDSON, *Associate Professor of Civil Engineering, Engineering Experiment Station, Iowa State College*

SYNOPSIS

PART I—IDENTIFICATION BY DIFFFRENTIAL THERMAL ANALYSIS

This paper is the first in a series of articles concerning the role of the clay fraction in engineering soils, including both the methods of analysis and the application of the results obtained therefrom to the determination and control of the engineering behavior of these soils. The differential thermal method of analysis is presented with the major emphasis on the preparation of samples for analysis so as to increase the sensitivity and accuracy of this analytical procedure.

Sample preparation becomes necessary whenever the clay fraction constitutes only a small percent of the soil or when other constituents are present whose reactions tend to mask those of the clay minerals. The clay concentration may be increased by extracting and analyzing either the soil fraction passing a 270 mesh sieve or the particles less than one micron in diameter. Interfering constituents may be eliminated by the proper treatment, e.g. the removal of organic material from a soil by the use of hydrogen peroxide.

Examples of the thermal patterns obtained by the use of these techniques in some Iowa soils are presented. These patterns are discussed to show what data can be obtained from this relatively simple, rapid method of soil analysis.

PART II—PARTICLE SIZE DISTRIBUTION AND CATION EXCHANGE CAPACITY

This is the second in a series of studies concerning the definition and control of the properties of the clay fraction in engineering soils. This article presents methods for the determination of the particle size distribution down to one-tenth micron diameter and below, and for the rapid determination of cation exchange capacity for the whole soil and for the less than one micron fraction. The methods presented have been selected because of their rapidity and simplicity and because they employ equipment which is readily available.

Correlation of the results obtained by these methods cannot at the present be made with soil properties except in a very general manner. However, these methods are accurate and when the basic knowledge relating fundamental clay properties and soil behavior is known they will be valuable analytical tools. Further studies with the purpose of making available the knowledge necessary for the fullest application of analytical research to practical engineering are in progress.

PART I—IDENTIFICATION BY DIFFERENTIAL THERMAL ANALYSIS

It is now well established that the clay fraction of soil is the seat of varied and vigorous reactions which greatly influence the behavior of soil as an engineering material. Experimental evidence indicates that such properties as plasticity, adsorption, shrinkage,